A Simple Route for the Preparation of Mesoporous Nanostructures Using Block Copolymers

Dian Chen,[†] Soojin Park,[‡] Jiun-Tai Chen,[†] Emily Redston,[§] and Thomas P. Russell[†,*]

[†]Department of Polymer Science and Engineering, University of Massachusetts, Amherst, Massachusetts 01003, [‡]School of Energy Engineering, Ulsan Institute of Science and Technology, Ulsan, Korea, and [§]Department of Material Science and Engineering, Cornell University, Ithaca, New York 14853

ABSTRACT Poly(styrene-*b*-4-vinylpyridine) (PS-*b*-P4VP) nanostructures with multiple morphologies were fabricated by immersing PS-*b*-P4VP nanotubes in ethylene glycol, a nonsolvent for PS and a good solvent for P4VP, at different temperatures. Mesoporous structures were generated from uniform nanoscopic wormlike micelles due to a solvent-induced reconstruction when the spherical micellar structures were heated above the glass transition temperature of the PS block. The mesoporous nanostructures can be converted into inorganic oxide structures, like SiO_2 and TiO_2, by well-known sol—gel methods. The mesoporous inorganic oxides can be produced with tunable porosity by controlling the molecular weight of the block copolymers. Confinement also plays an important role to create the nanostructures with unusual morphologies.

KEYWORDS: block copolymer · ethylene glycol · mesoporous structure · morphologies · nanotube(s)

During the last two decades, mesoporous materials have been of great interest due to their potential applications, including filtration, catalysis, adsorption, and reactive separation processes.[1−5] Mesoporous inorganic materials, such as inorganic oxide ceramics, are widely used as filters for the mechanical and biological treatment of liquids in the food and pharmaceutical industry and for capturing precious or toxic components in eluents.[6−8] However, most studies on mesoporous materials have focused on materials fabricated in the bulk or thin films.[9,10] There are fewer studies on the generation of mesoporous inorganic nanoscopic materials as, for example, nanorods or nanotubes, which have distinct advantages for the specialized purposes of energy conversion and molecular sensory devices. Generating polymer nanoscopic materials having rationally designed mesoporous structures or surface topographies still remains a challenge.

Block copolymers (BCPs) have received much attention due to their ability to self-assemble, both in the bulk and in confined geometries, into a range of nanoscopic morphologies, including spherical, cylindrical, lamellar, and gyroid morphologies, depending on the volume fraction of the components.[11,12] The directed self-assembly of BCPs into arrays of spherical or cylindrical microdomains having long-range lateral ordering has received considerable attention as templates and scaffolds for the fabrication of high-density arrays of nanoscopic elements that could be used in data storage,[12] electronics,[13] and molecular separation.[14] Equally attractive are the abilities to control the size of the nanoscopic microdomains and the areal density of the arrays by varying the molecular weight of the BCP and to manipulate their functionality.[12,14,15] Most studies on the self-assembly of BCPs have focused on planar surfaces, with little effort on curved surfaces or the manner in which curvature can influence the microphase separation of the BCPs. Recently, the self-assembly of BCPs in confined geometries, for example, nanotubes, nanorods, and nanofibers, has attracted more attention. These nanostructures have been made by various methods, such as templating,[16−19] self-assembly,[20−22] and electrospinning.[23,24] By using templates, such as anodized aluminum oxide (AAO) membranes, BCP nanorods and nanotubes have been generated inside the cylindrical nanopores of the templates. By using a weak acid or weak base to dissolve the membrane, the nanorods or nanotubes can be isolated for subsequent use and analysis. Cylindrical confinement plays an important role in determining the BCP morphologies which depend on the pore diameter and the interfacial interactions.[25] In particular, helical nanostructures were fabricated by self-assembly of BCP melts or sol solutions containing BCP templates

*Address correspondence to russell@mail.pse.umass.edu.

Received for review July 10, 2009 and accepted August 17, 2009.

Published online August 31, 2009.
10.1021/nn900782k CCC: $40.75

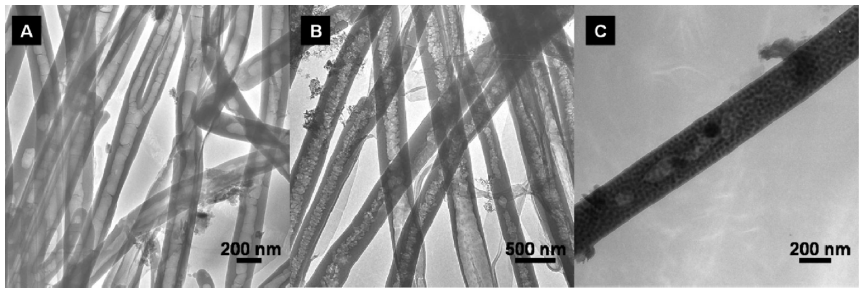

Figure 1. TEM micrographs of PS(47.6k)-*b*-P4VP(20.9k) nanotubes prepared using an AAO membrane as a template: (A) without THF vapor treatment, (B) after THF vapor treatment, but no I_2 staining, and (C) after THF vapor treatment, and stained with I_2.

inside the nanochannels.[26,27] In this paper, helically organized micelles were obtained as the result of confined reconstruction in ethylene glycol, but the mechanism lacks theoretical predictions.

Solvent reconstruction of BCPs is a simple, nondestructive method to produce nanoporous templates in thin films without changing the original spatial organization of the BCP.[28,29] Solvent reconstruction is a process where, in the case of thin films, the films are immersed in a solvent that is a good solvent for the minor component block and a nonsolvent for the major component. If the major component is below its glass transition temperature (T_g) during solvent exposure, the solvent solubilizes the minor component, drawing the minor component to the surface with the constraint that the minor component chain is still covalently linked to the matrix. With cylindrical microdomains oriented normal to the film surface, this reconstruction results in the formation of nanopores with the minor component block fully covering the surface of the thin film. Park *et al.*[29] demonstrated that highly oriented cylindrical microdomains with long-range lateral order can be achieved in thin films of poly(styrene-*b*-4-vinylpyridine) (PS-*b*-P4VP) by spin-coating the copolymer from a mixed solvent (toluene/THF). After dipping the films into ethanol, a preferential solvent for P4VP, a nanoporous film was produced, leaving P4VP on the surface. Just as important is the fact that heating the reconstructed film above the T_g of the minor component block restores the film to its original state. Consequently, the solvent reconstruction is fully reversible. Chen *et al.*[19] made porous poly(styrene-*b*-ethylene oxide) (PS-*b*-PEO) nanotubes by selectively swelling the PEO cylindrical domains using water/methanol mixtures. Recently, Steinhart *et al.*[30] fabricated multiple nanoscopic architectures by swelling the P2 VP domain in PS-*b*-P2 VP rods prepared in AAO templates. All of these studies have focused on reconstruction processes where the matrix component is below its T_g. Here, on the other hand, we focus on nanotubes where the matrix component is above its T_g and, as such, impart significant mobility to this block that enables a complete reconstruction of the nanotube into unusual morphologies.

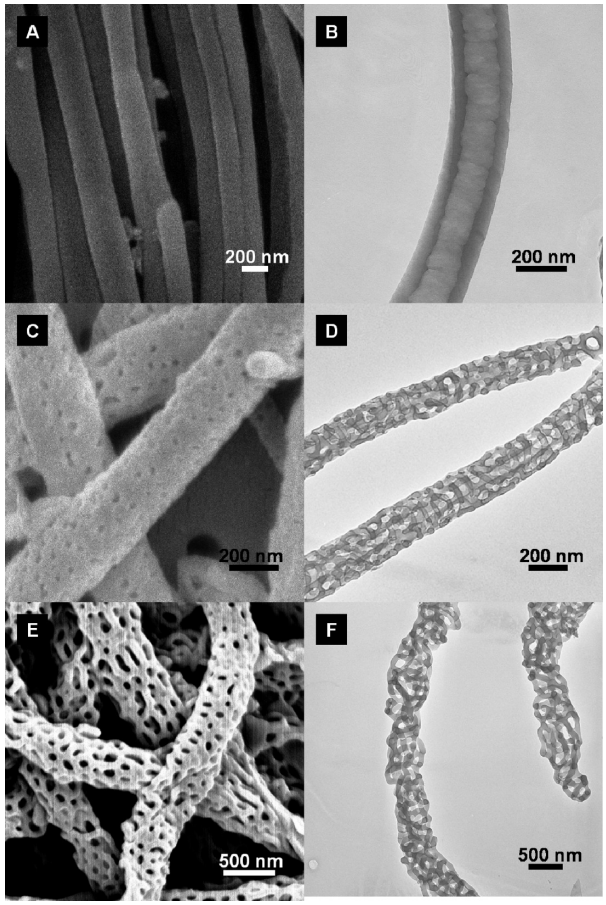

Figure 2. Electron micrographs of PS(47.6k)-*b*-P4VP(20.9k) nanotubes after suspension in ethylene glycol at different temperatures: (A) scanning electron microscopy (SEM) image of the tubes after suspension for 1 h at room temperature, (B) TEM image of the tubes after suspension for 1 h at room temperature, (C) SEM image of the tubes after suspension for 5 min at 95 °C, (D) TEM image of the tubes after suspension for 5 min at 95 °C, (E) SEM image of the tubes after suspension for 5 min at 130 °C, and (F) TEM image of the tubes after suspension for 5 min at 130 °C.

PS-*b*-P4VP nanotubes were prepared by filling an AAO membrane with the BCP chloroform solution and allowing the solvent to evaporate, leaving a thin layer of the BCP on the walls of the nanopores to form nanotubes. The PS-*b*-P4VP nanotubes confined within the AAO membrane were exposed to tetrahydrofuran (THF) vapor, a good solvent for PS but a nonsolvent for P4VP, to generate uniform and spherical micelles along the tube wall. The AAO membrane was then dissolved in 5 wt % $NaOH_{(aq)}$, and the nanotubes were released and filtered. The nanotubes were dried for 1 day and then suspended in ethylene glycol, a preferential solvent for P4VP, at elevated temperatures. At temperatures above the T_g of PS (~100 °C), the mobility of the PS, coupled with the solvation of the P4VP block, resulted in a range of different morphologies that spanned multiple length scales. These morphologies can also be converted to

mesoporous inorganic oxides by complexing precursors, like tetraethyl orthosilicate or titanium tetraethoxide, with the vinylpyridine. This process offers a simple route for the fabrication of tunable mesoporous ceramic or metallic structures that can be controlled by changing molecular weight and volume fraction of the BCPs.

RESULTS AND DISCUSSION

Figure 1 shows transimission electron microscopy (TEM) images of PS(47.6k)-*b*-P4VP(20.9k) nanotubes before and after the solvent annealing inside the AAO membrane. PS-*b*-P4VP nanotubes shown in Figure 1A were prepared after the polymer solution was drawn into the AAO membrane by capillary force, followed by solvent evaporation. When the PS-*b*-P4VP nanotubes confined in the AAO membrane were exposed to THF vapor, a slightly selective solvent for PS, at room temperature for 6 h, uniform spherical micellar structures formed along the nanotubes (Figure 1B,C). Subsequently, the AAO template was dissolved in 5 wt % $NaOH_{(aq)}$ for 1 h and washed three times with water to release the PS-*b*-P4VP nanostructures. For TEM measurements, the samples were then sonicated in water for 2 min, placed onto Formvar-coated copper grids, and stained with iodine (I_2) vapor for 7 h. Figure 1A,B shows the tubular structures with and without THF vapor treatment. As shown in Figure 1C, uniform micellar structures are seen after solvent annealing since I_2 preferentially stained the P4VP.

After dissolving the AAO template, the nanotubes were washed three times with deionized water then redispersed in ethylene glycol. Ethylene glycol, with a relatively high boiling point of 197.3 °C, is a selective solvent for the P4VP block at sufficiently high temperatures. Since ethylene glycol has a high viscosity (η = 16.1 mPa · s) at room temperature, it does not offer sufficient mobility to the P4VP to affect a change. When the THF-annealed PS-*b*-P4VP tubes were released from the AAO template and suspended in ethylene glycol at room temperature for 1 h, no swelling took place and, as shown in Figure 2A,B, the tubular structures were maintained, and the surface remained smooth. When the nanotube suspension was heated to 95 °C (just below the glass transition temperature of PS) for only 5 min, a solvent-induced surface reconstruction of the nanotubes occurred. At 95 °C, the viscosity of ethylene glycol decreased substantially ($\eta \approx$ 1.98 mPa · s) and swelled the P4VP, while the PS remained in the glassy state. Upon drying, porous nanotubes had been developed, as shown in Figure 2C,D.

When the PS-*b*-P4VP nanotubes were exposed to ethylene glycol at 130 °C, well above the glass transition temperature of PS, substantial structural changes occurred, as shown in Figure 2E,F. Uniform wormlike micelles, having a diameter of ~73 nm, were entangled with each other to form a mesoporous nanostructure

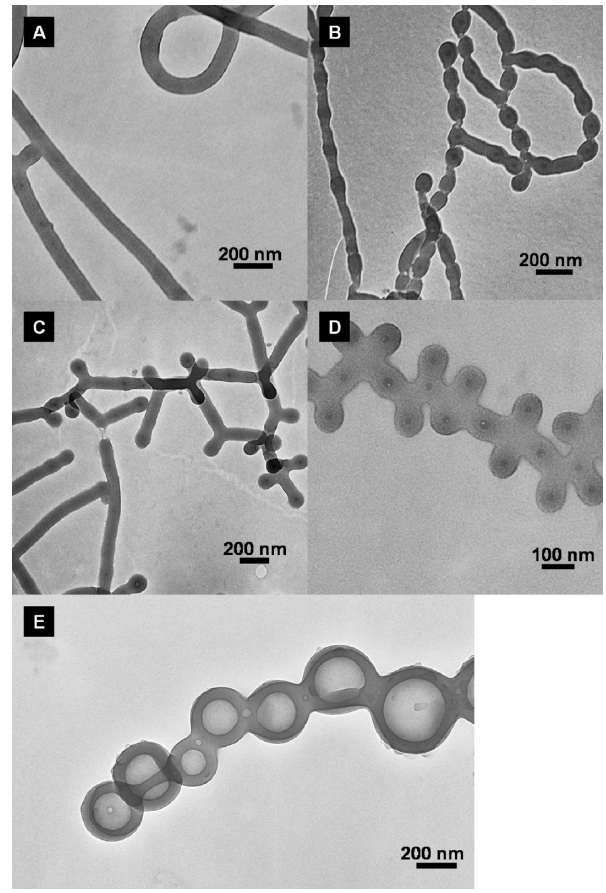

Figure 3. Electron micrographs of PS(47.6k)-*b*-P4VP(20.9k) nanotubes after suspension in ethylene glycol at 170 °C for different periods of time: (A) TEM image of the tubes after suspension for 5 min, (B) TEM image of the tubes after suspension for 10 min, (C) TEM image of the tubes after suspension for 30 min, (D) TEM image of the tubes after suspension for 2 h, and (E) TEM image of the tubes after suspension for 3 h.

with an average pore diameter of ~80 nm. It should be noted that the repeat period of the PS-*b*-P4VP in the bulk is 36.4 nm.[29] Since the P4VP chains that formed the core in the spherical micelle were drawn out by the selective solvent ethylene glycol and the PS is mobile at this temperature, P4VP in adjacent domains can merge, resulting in the observed wormlike micellar structures with P4VP as the corona. The diameters of nanostructures in Figure 2E,F are nearly twice that of the nanotubes in Figure 1. It should be noted that much more void volume formed when the wormlike micelles begin to intermesh.

When the PS-*b*-P4VP nanotubes were exposed to ethylene glycol at 170 °C, much higher than the T_g's of both blocks, disentangled strands, ~73 nm in diameter, were produced, even with a suspension time of only 5 min. The outer layers of the strands are P4VP, due to the preferential solvation in ethylene glycol. As shown in Figure 3A, strands with darker outer layers (P4VP) were seen after I_2 staining. When the suspension time was increased to 10 min, Rayleigh instabilities were observed in the wormlike micelles, reducing the total surface area.[31] Consequently, the surfaces undulated and regu-

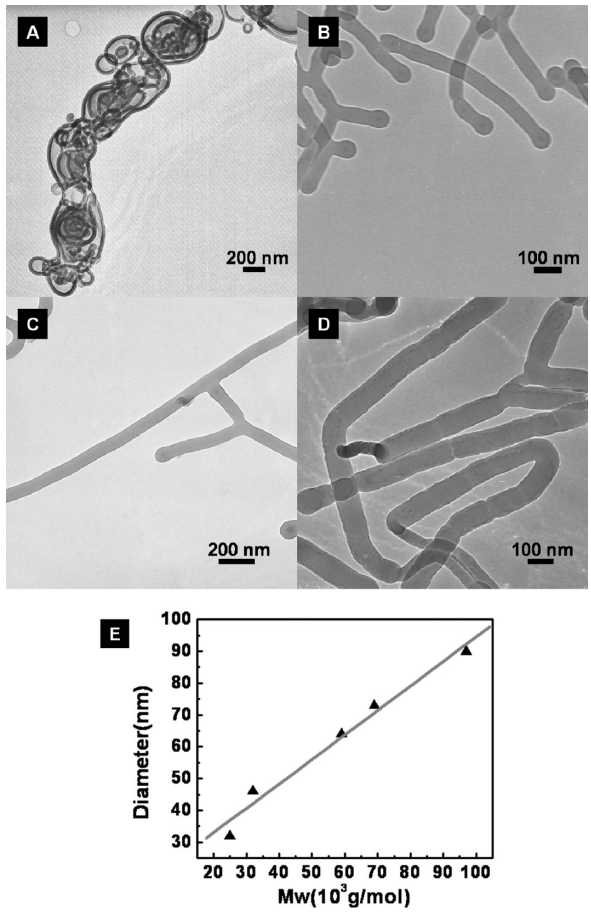

Figure 4. TEM images of PS-*b*-P4VP nanotubes with different molecular weight after suspension in ethylene glycol for 5 min at 170 °C: (A) PS(21k)-*b*-P4VP(4k), (B) PS(25k)-*b*-P4VP(7k), (C) PS(41.5k)-*b*-P4VP(17.5k), (D) PS(72k)-*b*-P4VP(25k), and (E) the diameters of the single strands *vs* the molecular weight of BCPs.

larly spaced spheres formed along the wormlike micelle (Figure 3B). Quere *et al.*[32] have reported similar instabilities when polymer films were coated on a fiber. Some branches are also shown in Figure 3B. When the suspension time was further increased to 30 min, the branches were shortened (Figure 3C), as some spheres in the branched micelles (Figure 3B) were detached from the system to further reduce the surface energy. Similar branched cylindrical micelles were observed by Liu *et al.*[20]

When the suspension time was increased to 2 h, flower-type structures formed, as shown in Figure 3D. An equilibrium state was reached when the suspension time was increased to 3 h, and vesicular structures formed (Figure 3E), reducing the surface area and core-chain stretching.[33]

The influence of BCP molecular weight on the morphologies was investigated using five different cylinder forming PS-*b*-P4VP BCPs. As described above, polymer nanotubes were prepared and solvent annealed to produce regular spherical micellar arrays inside the AAO membrane. Subsequently, they were suspended in ethylene glycol for different temperatures and times.

Regardless of BCP molecular weights, results similar to the PS(47.6k)-*b*-P4VP(20.9k) described above were obtained. When the tubes were suspended at 130 °C for 5 min, mesporous tubes were formed. The only difference was that the diameters of the entangled wormlike micelles depended on the BCP molecular weight. When the PS-*b*-P4VP nanotubes (~200 nm in diameter) were exposed to ethylene glycol at 170 °C, the mesoporous tubes disentangled to form single wormlike micelles, with a diameter that increased linearly with molecular weight. The diameters of the wormlike micelles of PS(21k)-*b*-P4VP(4k), PS(25k)-*b*-P4VP(7k), PS(41.5k)-*b*-P4VP(17.5k), and PS(72k)-*b*-P4VP(25k) were 32, 46, 64, and 90 nm, respectively (Figures 4A−D).

To investigate the influence of confinement on the morphologies of the swollen BCPs, the solvent-annealed PS(47.6k)-*b*-P4VP(20.9k) nanotubes confined in the AAO membranes were immersed in the ethylene glycol, and the temperature was increased to 130 °C for different annealing times. After annealing, the samples were cooled and the AAO template was removed using 5 wt % $NaOH_{(aq)}$, releasing the nanostructures. Electron micrographs of the nanostructures are shown in Figure 5. Similar to the structures shown in Figure 2C,D, the solvent-induced reconstruction began at the inner surface of the nanotubes when annealed at 130 °C for 5−30 min. The P4VP was drawn out by ethylene glycol, leaving porous structures behind (Figure 5A,B), but the reconstruction was much slower when the nanotubes were confined. When the annealing time was increased to 3 h, the P4VP in the adjacent domains began to merge and interconnect, forming wormlike micellar structures with P4VP as the corona and PS as the core. The diameter of these micelles is ~73 nm, as shown in Figure 5C. Figure 5D shows that the wormlike micelles formed around the center of the nanotubes, due to the confinement, when the tubes were annealed for 5 h. Such helical micelles are unusual templates that can be converted into inorganic oxide structures by a sol/gel replication method.

The confinement also forced the tube size to remain equal to that of the nanopore, in contrast to those shown in Figure 2E,F, where the nanotube diameters increased significantly.

The mesoporous PS-*b*-P4VP structures produced by these annealing processes were also used as scaffolds to generate corresponding silica and titania nanostructures. Copper grids covered with the PS-*b*-P4VP mesoporous nanostructures shown in Figure 2E,F were immersed in a hydrolyzed precursor solution (silica or titania precursor) for 10 min to let the precursor complex with P4VP chains. The grids were then washed in ethanol for several seconds to remove excess sol precursor. Subsequently, the copper grids were heated to 400 °C in air for 1 h to remove the BCP surfactant, leaving only silica or titania, templated by the BCP. The SEM images of

these silica and titania nanostructures are shown in Figure 6A,C, respectively. The entangled fibrillar networks are seen to be hollow in the TEM images (Figure 6B,D) because P4VP constitutes the corona of the wormlike micelles. Consequently, by this strategy, mesoporous silica and titania materials having novel morphologies can be generated. Using the same method, the silica and titania nanotubes with different diameters can be easily fabricated by using the nanostructures shown in Figures 3A and 4 as the scaffolds.

CONCLUSION

The fabrication of PS-*b*-P4VP tubes with a variety of morphologies in ethylene glycol at different suspension temperatures and times and confinement conditions was investigated. The solvent-induced reconstruction process in ethylene glycol, a preferential solvent for P4VP chains, can be used at temperatures above and below the T_g of the PS block, enabling significant flexibility in manipulating the morphologies. At 95 °C, slightly below the T_g of PS, porous polymeric nanotubes were obtained. At 130 °C, above the glass transition temperature of PS, the fibers consisting of entangled uniform nanoscopic wormlike micelles were formed. Such mesoporous structures can be used as scaffolds to produce silica and titania replicas, using a sol−gel method. At much higher temperatures, such as 170 °C, single wormlike micelles with fixed diameters formed at short annealing times. With increasing time, Rayleigh instabilities occurred, producing regularly spaced spheres along the wormlike micelle. The diameter of the wormlike micelle increased linearly with the molecular weight of the BCPs. When the solvent-annealed polymeric nanotubes confined within the AAO membranes were immersed in the ethylene glycol, markedly different morphologies were obtained that could be also used as scaffolds for silica and titania nanostructures. While the unusual morphologies observed by these reconstruction processes are of fundamental interest, the reconstructed block copolymer tubes could also be used as substrates for atomic layer deposition.[26,34] The morphologies and the ability to convert these reconstructed block copolymer tubes into silica and titania have interesting applictions ranging from filtration media to nanocomposite materials to photovoltaics.

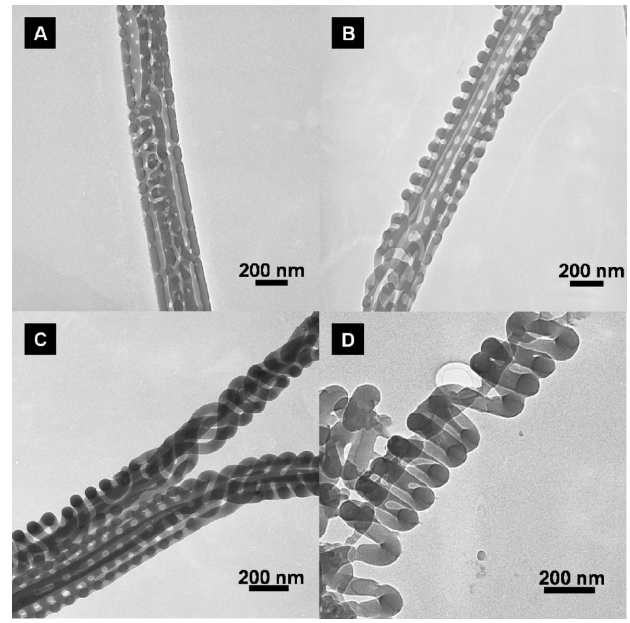

Figure 5. Electron micrographs of PS(47.6k)-*b*-P4VP(20.9k) nanotubes confined in AAO after immersed in ethylene glycol at 130 °C for different periods of time: (A) TEM image of a nanotube after immersed for 5 min, (B) TEM image of nanotubes after immersed for 30 min, (C) TEM image of nanotubes after immersed for 3 h, (D) TEM image of nanotubes after immersed for 5 h. AAO membranes were removed after immersed in ethylene glycol.

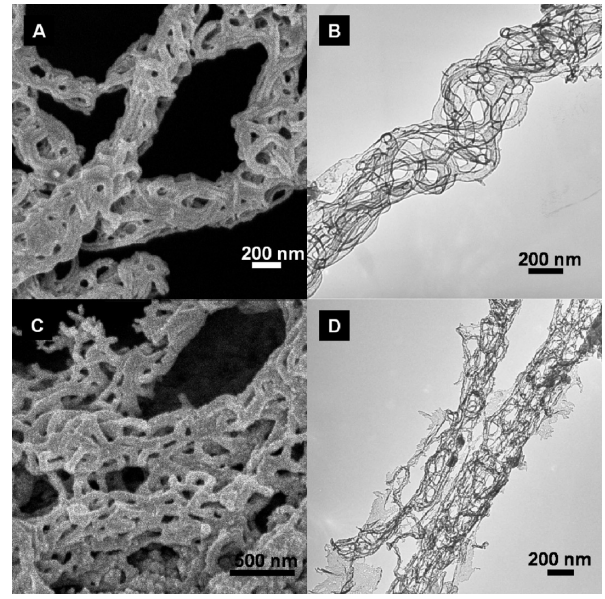

Figure 6. Electron micrographs of mesoporous ceramics prepared from PS(47.6k)-*b*-P4VP(20.9k) mesoporous nanostructures shown in Figure 2E,F: (A) SEM image of the mesoporous silica tubes, (B) TEM image of the mesoporous silica tubes, (C) SEM image of the mesoporous titania tubes, and (D) TEM image of the mesoporous titania tubes.

EXPERIMENTAL SECTION

Materials. Five different molecular weight PS-*b*-P4VPs were purchased from Polymer Source: PS(47.6k)-*b*-P4VP(20.9k) (M_n^{PS} = 47.6 kg/mol, M_n^{P4VP} = 20.9 kg/mol, with a total polydispersity (PDI) of 1.14); PS(72k)-*b*-P4VP(25k) with a PDI of 1.09; PS(41.5k)-*b*-P4VP(17.5k) with a PDI of 1.07; PS(25k)-*b*-P4VP(7k) with a PDI of 1.09; and PS(21k)-*b*-P4VP(4k) with a PDI of 1.2. Tetraethyl orthosilicate (TEOS, 98%) was purchased from Acros Organics, and titanium tetraethoxide (TEOT) was purchased from Alfa Aesar. The AAO membranes, having a thickness of ~60 μm and pore diameters of ~150−400 nm (an average pore diameter of 200 nm), were purchased from Whatman.

Preparation of Polymer Nanotubes and Mesoporous Nanostructures. The generation of polymer nanotubes inside the AAO membranes was described previously.[31,35] Three drops of PS-*b*-P4VP solution (5 wt %) in chloroform were placed on a glass slide. Subsequently, an AAO membrane was placed on top of the solution. The nanopores of the membrane were filled with the solution within a few seconds by capillary action, and the membrane turned transparent. After solvent evaporation at ambient conditions, thin PS-*b*-P4VP layers were deposited onto the walls of nanopores in the membrane, resulting in the formation of nanotubes. The membranes with the nanotubes were further dried at 45 °C under vacuum overnight to completely remove the residual solvent. Then the PS-*b*-P4VP nanotubes confined within the AAO membrane were exposed to tetrahydrofuran (THF) vapor for 6 h. The AAO membrane was then dissolved in 5 wt % $NaOH_{(aq)}$, and the nanotubes were released and filtered. The nanotubes were dried for 1 day and then suspended in ethylene glycol for different times at different temperatures.

Preparation of Mesoporous Ceramic Materials. For conversion to silica, a well-established synthetic process was used to produce a silica−surfactant sol.[36] At first, 2.08 g (0.01 mol) of tetraethyl orthosilicate (TEOS) was mixed with 3 g of HCl (0.2 M), 1.8 g of H_2O, and 5 mL of ethanol, and the stirred mixture was heated to 60 °C for 1.5 h to complete the acid-catalyzed hydrolysis−condensation of the silica precursor.[36] For the titania sol, 4.2 g of titanium tetraethoxide (TEOT) was mixed with 3.2 g of HCl (12.1 M), and the mixture was stirred vigorously at room temperature for 10 min, then 5 mL of ethanol was added. Copper grids covered with the PS-*b*-P4VP mesoporous nanostructures were immersed in the hydrolyzed precursor solution (silica precursor or titania precursor) for 10 min and washed in ethanol for a few seconds to remove excess sol precursor. Subsequently, the copper grids were heated to 400 °C in air for 1 h to remove the BCP surfactant. In so doing, the PS-*b*-P4VP mesoporous nanostructures were successfully replaced by silica or titania.

Characterization. A scanning electron microscope (SEM, JEOL 6320) with an accelerating voltage of 5 kV was used to investigate the nanostructures. All samples were coated with 5 nm of Au before performing SEM measurements. Bright field transmission electron microscopy (TEM) studies were conducted with a JEOL 2000 FX TEM operated at an accelerating voltage of 200 kV. For TEM, the samples were placed onto Formvar-coated copper grids.

Acknowledgment. This work was supported by the U.S. Department of Energy (DOE), and the NSF supported MRSEC at the University of Massachusetts Amherst. S.P. was supported by WCU (R31-2008-000-20012-0) programs.

REFERENCES AND NOTES

1. Kresge, C. T.; Leonowicz, M. E.; Roth, W. J.; Vartuli, J. C.; Beck, J. S. Ordered Mesoporous Molecular Sieves Synthesized by a Liquid-Crystal Template Mechanism. *Nature* **1992**, *359*, 710–712.
2. Tanev, P. T.; Pinnavaia, T. J. A Neutral Templating Route to Mesoporous Molecular Sieves. *Science* **1995**, *267*, 865–867.
3. Bagshaw, S. A.; Prouzet, E.; Pinnavaia, T. J. Templating of Mesoporous Molecular Sieves by Nonionic Polyethylene Oxide Surfactants. *Science* **1995**, *269*, 1242–1244.
4. Huo, Q. S.; Leon, R.; Petroff, P. M.; Stucky, G. D. Mesostructure Design with Gemini Surfactants: Supercage Formation in a Three-Dimensional Hexagonal Array. *Science* **1995**, *268*, 1324–1327.
5. Monnier, A.; Schuth, F.; Huo, Q.; Kumar, D.; Margolese, D.; Maxwell, R. S.; Stucky, G. D.; Krishnamurty, M.; Petroff, P.; Firouzi, A.; Janicke, M.; Chmelka, B. F. Cooperative Formation of Inorganic−Organic Interfaces in the Synthesis of Silicate Mesostructures. *Science* **1993**, *261*, 1299–1303.
6. Drev, D.; Vrhovsek, D.; Panjan, J. Using Porous Ceramics as a Substrate or Filter Media during the Cleaning of Sewage. *Strojniski Vestn. J. Mech. Eng.* **2006**, *52*, 250–263.
7. Kanagawa, T.; Qi, H. W.; Okubo, T.; Tokura, M. Biological Treatment of Ammonia Gas at High Loading. *Water Sci. Technol.* **2004**, *50*, 283–290.
8. Wegmann, M.; Michen, B.; Graule, T. Nanostructured Surface Modification of Microporous Ceramics for Efficient Virus Filtration. *J. Eur. Ceram. Soc.* **2008**, *28*, 1603–1612.
9. Bosc, F.; Ayral, A.; Albouy, P. A.; Datas, L.; Guizard, C. Mesostructure of Anatase Thin Films Prepared by Mesophase Templating. *Chem. Mater.* **2004**, *16*, 2208–2214.
10. Alberius, P. C. A.; Frindell, K. L.; Hayward, R. C.; Kramer, E. J.; Stucky, G. D.; Chmelka, B. F. General Predictive Syntheses of Cubic, Hexagonal, and Lamellar Silica and Titania Mesostructured Thin Films. *Chem. Mater.* **2002**, *14*, 3284–3294.
11. Park, M.; Harrison, C.; Chaikin, P. M.; Register, R. A.; Adamson, D. H. Block Copolymer Lithography: Periodic Arrays of $\sim 10^{11}$ Holes in 1 Square Centimeter. *Science* **1997**, *276*, 1401–1404.
12. Thurn-Albrecht, T.; Schotter, J.; Kastle, C. A.; Emley, N.; Shibauchi, T.; Krusin-Elbaum, L.; Guarini, K.; Black, C. T.; Tuominen, M. T.; Russell, T. P. Ultrahigh-Density Nanowire Arrays Grown in Self-Assembled Diblock Copolymer Templates. *Science* **2000**, *290*, 2126–2129.
13. Fan, H. J.; Werner, P.; Zacharias, M. Semiconductor Nanowires: From Self-Organization to Patterned Growth. *Small* **2006**, *2*, 700–717.
14. Fasolka, M. J.; Mayes, A. M. Block Copolymer Thin Films: Physics and Applications. *Annu. Rev. Mater. Res.* **2001**, *31*, 323–355.
15. Hawker, C. J.; Russell, T. P. Block Copolymer Lithography: Merging "Bottom-Up" with "Top-Down" Processes. *MRS Bull.* **2005**, *30*, 952–966.
16. Shin, K.; Xiang, H. Q.; Moon, S. I.; Kim, T.; McCarthy, T. J.; Russell, T. P. Curving and Frustrating Flatland. *Science* **2004**, *306*, 76.
17. Xiang, H. Q.; Shin, K.; Kim, T.; Moon, S. I.; McCarthy, T. J.; Russell, T. P. Block Copolymers under Cylindrical Confinement. *Macromolecules* **2004**, *37*, 5660–5664.
18. Sun, Y. M.; Steinhart, M.; Zschech, D.; Adhikari, R.; Michler, G. H.; Gosele, U. Diameter-Dependence of the Morphology of PS-*b*-PMMA Nanorods Confined within Ordered Porous Alumina Templates. *Macromol. Rapid Commun.* **2005**, *26*, 369–375.
19. Chen, J. T.; Zhang, M. F.; Yang, L.; Collins, M.; Parks, J.; Avallone, A.; Russell, T. P. Templated Nanostructured PS-*b*-PEO Nanotubes. *J. Polym. Sci., Part B* **2007**, *45*, 2912–2917.
20. Stewart, S.; Liu, G. Block Copolymer Nanotubes. *Angew. Chem., Int. Ed.* **2000**, *39*, 340–344.
21. Hamley, I. W. Nanoshells and Nanotubes from Block Copolymers. *Soft Matter* **2005**, *1*, 36–43.
22. Raez, J.; Manners, I.; Winnik, M. A. Nanotubes from the Self-Assembly of Asymmetric Crystalline-Coil Poly(ferrocenylsilane-siloxane) Block Copolymers. *J. Am. Chem. Soc.* **2002**, *124*, 10381–10395.
23. Ruotsalainen, T.; Turku, J.; Heikkila, P.; Ruokolainen, J.; Nykanen, A.; Laitinen, T.; Torkkeli, M.; Serimaa, R.; ten Brinke, G.; Harlin, A.; Ikkala, O. Towards Internal Structuring of Electrospun Fibers by Hierarchical Self-Assembly of Polymeric Comb-Shaped Supramolecules. *Adv. Mater.* **2005**, *17*, 1048–1052.
24. Kalra, V.; Kakad, P. A.; Mendez, S.; Ivannikov, T.; Kamperman, M.; Joo, Y. L. Self-Assembled Structures in Electrospun Poly(styrene-*block*-isoprene) Fibers. *Macromolecules* **2006**, *39*, 5453–5457.
25. Yu, B.; Sun, P. C.; Chen, T. H.; Jin, Q. H.; Ding, D. T.; Li, B. H.; Shi, A. C. Confinement-Induced Novel Morphologies of Block Copolymers. *Phys. Rev. Lett.* **2006**, *96*, 138306(1)−138306(2).
26. Wang, Y.; Qin, Y.; Berger, A.; Yau, E.; He, C.; Zhang, L.; Gösele, U.; Knez, M.; Steinhart, M. Nanoscopic Morphologies in Block Copolymer Nanorods as Templates for Atomic-Layer Deposition of Semiconductors. *Adv. Mater.* **2009**, *21*, 2763–2766.
27. Wu, Y. Y.; Cheng, G. S.; Katsov, K.; Sides, S. W.; Wang, J. F.; Tang, J.; Fredrickson, G. H.; Moskovits, M.; Stucky, G. D. Composite Mesostructures by Nano-Confinement. *Nat. Mater.* **2004**, *3*, 816–822.

28. Xu, T.; Stevens, J.; Villa, J. A.; Goldbach, J. T.; Guarim, K. W.; Black, C. T.; Hawker, C. J.; Russell, T. R. Block Copolymer Surface Reconstuction: A Reversible Route to Nanoporous Films. *Adv. Funct. Mater.* **2003**, *13*, 698–702.
29. Park, S.; Wang, J. Y.; Kim, B.; Chen, W.; Russell, T. P. Solvent-Induced Transition from Micelles in Solution to Cylindrical Microdomains in Diblock Copolymer Thin Films. *Macromolecules* **2007**, *40*, 9059–9063.
30. Wang, Y.; Gosele, U.; Steinhart, M. Mesoporous Block Copolymer Nanorods by Swelling-Induced Morphology Reconstruction. *Nano Lett.* **2008**, *8*, 3548–3553.
31. Chen, J. T.; Zhang, M. F.; Russell, T. P. Instabilities in Nanoporous Media. *Nano Lett.* **2007**, *7*, 183–187.
32. Quere, D.; Dimeglio, J. M.; Brochardwyart, F. Spreading of Liquids on Highly Curved Surfaces. *Science* **1990**, *249*, 1256–1260.
33. Soo, P. L.; Eisenberg, A. Preparation of Block Copolymer Vesicles in Solution. *J. Polym. Sci., Part B* **2004**, *42*, 923–938.
34. Ras, R. H. A.; Kemell, M.; de Wit, J.; Ritala, M.; ten Brinke, G.; Leskela, M.; Ikkala, O. Hollow Inorganic Nanospheres and Nanotubes with Tunable Wall Thicknesses by Atomic Layer Deposition on Self-Assembled Polymeric Templates. *Adv. Mater.* **2007**, *19*, 102–106.
35. Chen, D.; Chen, J. T.; Glogowski, E.; Emrick, T.; Russell, T. P. Thin Film Instabilities in Blends under Cylindrical Confinement. *Macromol. Rapid Commun.* **2009**, *30*, 377–383.
36. Platschek, B.; Petkov, N.; Bein, T. Tuning the Structure and Orientation of Hexagonally Ordered Mesoporous Channels in Anodic Alumina Membrane Hosts: A 2D Small-Angle X-ray Scattering Study. *Angew. Chem., Int. Ed.* **2006**, *45*, 1134–1138.